

Theoretical study on β -aminoacroleine; Density functional theory, atoms in molecules theory and natural bond orbitals studies

HEIDAR RAISSI, MEHDI YOOSEFIAN*, EFFAT MOSHFEGHI and FARZANEH FARZAD
Chemistry Department, Birjand University, Birjand 97175-615, Iran
e-mail: myoosefian@yahoo.com; hraissy@yahoo.com

MS received 13 July 2011; revised 22 September 2011; accepted 31 October 2011

Abstract. The characteristics of the intramolecular hydrogen bonding for a series of 19 different derivatives of β -aminoacroleine have been systematically analysed at the B3LYP/6-31G** level of theory. The topological properties of the electron density distributions for N–H \cdots O intramolecular bridges have been analysed by the Bader theory of atoms in molecules. The electron density (ρ) and Laplacian ($\nabla^2\rho$) properties at critical points of the relevant bonds, estimated by AIM calculations, showed that N–H \cdots O have low and positive character ($\nabla^2\rho > 0$), consistent with electrostatic character of the hydrogen bond. The vibrational study of the hydrogen bonded systems showed negative (red) shifts for the $\nu_{\text{N-H}}$ stretching mode. The π -electron delocalization parameter (Q) as a geometrical indicator of a local aromaticity and the geometry-based HOMA have also been calculated. Furthermore, the analysis of hydrogen bond in this molecule and its derivatives by natural bond orbital (NBO) methods support the DFT results. The results of AIM and NBO analysis as well as $\nu_{\text{N-H}}$ were further used for estimation of the hydrogen bonding interactions and the forces driving their formation. The various correlations were found between geometrical, energetic and topological parameters. The substituent effect was also analysed and it was found that the strongest hydrogen bonds exist for N⁺(CH₃)₃ and Cl substituents while the weakest ones for COOCH₃.

Keywords. β -Aminoacroleine; intramolecular hydrogen bond; NBO; AIM and harmonic oscillator model of aromaticity index (HOMA).

1. Introduction

Hydrogen bonds (HBs) play major roles in influencing the structure and behaviour of organic and inorganic compounds and biomolecules, in molecular processes, and in chemical reactivity.^{1–12} Hydrogen bonding may also play an important role in the biomedical activity of some drugs. The intramolecular hydrogen bonding (HB) is the particular case of the above mentioned interaction. It is formed by different parts of the same molecule or ion and its existence leads to the creation of the so-called quasi-ring. In aminoketone compounds, intramolecular hydrogen bonding is displayed between the two electronegative atoms, which are designated proton donors and proton acceptors. These compounds are sample of molecules where some of the shortest intramolecular hydrogen bonding distances occur. β -aminoacroleine (AMAC) is the simplest of aminoketone compounds. AMAC has been studied extensively not only because of the system's biological connections, but also it is the prototypical model for intramolecular hydrogen bonding.

The β -aminoacroleine is an interesting molecule, which involved in N–H \cdots O and O–H \cdots N intramolecular hydrogen bonds. Furthermore, this compound is capable of forming tautomeric equilibria between ketoamine, ketoimine and enolimine. AMAC resembles malonaldehyde in that it has NH₂ group instead of an OH group. This molecule plays a similar role in the chemistry of β -ketoamines, as malonaldehyde does in the chemistry of β -dicarbonyls.¹³ The results of the calculations show that AMAC has a relatively strong intramolecular hydrogen bond with a N \cdots O distance of 2.693 Å.

Special attention is often given to strong intramolecular H-bonds and the so-called resonante-assisted hydrogen bonds (RAHBs). It seems that AMAC molecule has a π -electron delocalization of the O=C–C=C–NHR carbonyl-amine group. According to the statements of Gilli *et al.*¹⁴ such a π -electron delocalization is responsible for the changes of geometry of the skeleton constituting the space between the H-bonds donor and acceptor.

Our theoretical calculations demonstrate that the hydrogen bond strength increases when one of the hydrogen atoms on the nitrogen atom of AMAC is

*For correspondence

substituted by groups such as $-\text{NO}_2$, $-\text{Cl}$, $-\text{CF}_3$, $-\text{F}$, $-\text{Br}$, $-\text{Ph}(\text{ParaOCH}_3)$, etc. This is true except for bulky groups such as $-\text{CHO}$, $-\text{C}(\text{CH}_3)_3$ and $-\text{Si}(\text{CH}_3)_3$. Spectroscopy studies^{15,16} showed that in the case where CH_3 (an electron-releasing group), is substituted instead of the hydrogen atom (on NH_2 group), varies the chemical properties of compound.

Such molecules are very interesting from a theoretical point of view because the hydrogen bond strength nearly originates exclusively from steric effects, given that the nearly perpendicularity of the substituent and the ring prevents conjugation. The study of β -aminoacroleine derivatives, with N-substituting groups of different dimensions, would cause the different effects due to conjugation and steric hindrance both on the molecular structure and on the hydrogen bridge to be emphasized (see figure 1).

In this work, we investigated the following compounds: **1**, N,N,N-Trimethyl-N'-(3-oxo-propenyl)-hydrazinium, **2**, 3-amino-ethynyleamino-propenal, **3**, 3-Bromoamino-propenal, **4**, 4-Trifluoromethylamino-propenal, **5**, 3-Methylamino-propenal, **6**, 3-Chloroamino-propenal, **7**, N-(3-oxo-propenyl)-formamide, **8**, 3-Ethylamino-propenal, **9**, 3-Fluoroamino-propenal, **10**, 3-Hydrazino-propenal, **11**, 3-Nitroamino-propenal, **12**, 3-Methoxyamino-propenal, **13**, 3-Ethoxyamino-propenal, **14**, 3-Hydroxyamino-propenal, **15**, 3-(4-Nitro-phenylamino)-propenal, **16**, 3-(4-Methoxy-phenylamino)-propenal, **17**, 3-Phenylamino-propenal, **18**, 3-(Trimethylsilylamino)-propenal, **19**, 3-tert-Butylamino-propenal (the abbreviations and substitution position are depicted in figure 1). Among the AMAC derivatives, compounds **2–16** would have negligible steric hindrance, while in **1, 19** the steric hindrance is very strong.

The aim of the present paper is the theoretical investigation of β -aminoacroleine and its derivatives in order to account for the role of the R substitution on the structure, strength of the $\text{N}-\text{H}\cdots\text{O}$ hydrogen bridge and to

estimate the energy of the $\text{N}-\text{H}\cdots\text{O}$ hydrogen bonds. In order to rationalize the effects of each substituent group on the hydrogen bond energy (E_{HB}) of the parent molecule and the cumulative effects of substitution on the hydrogen bond, energy of AMAC were taken into account.

2. Computational methods

All the calculations on AMAC and its derivatives have been performed using GAUSSIAN98 series of programs.¹⁷ Geometry optimizations were carried out at B3LYP/6-31G** level of theory.¹⁸ Vibrational frequencies for all derivatives were calculated at the same level of theory. In assigning the calculated frequencies to approximate vibrational descriptor, the vibrational modes have been analysed by means of the atom movements, calculated in Cartesian coordinates.

The nature of the intramolecular hydrogen bonds existing within AMAC derivatives were studied by means of the Bader theory of atoms in molecules (AIM). According to this theory, when two neighbouring atoms are chemically bonded, a critical point for bond formation appears between them. At the bond critical point, $\nabla^2\rho = 0$, the charge density is minimum at r_c along the bond path but maximum along any orthogonal displacement. The sign of Laplacian for electron density at a bond critical point, $\nabla^2\rho$, reveals whether the charge is concentrated, as in covalent bond ($\nabla^2\rho < 0$), or depleted, as in closed shell (electrostatic) interactions ($\nabla^2\rho > 0$). The calculated electron density, ρ , and its second derivative, $\nabla^2\rho$ were used for describing the nature of the intramolecular $\text{N}-\text{H}\cdots\text{O}$ bonds. The AIM calculations were performed on the B3LYP/6-31G** wave function using the critical point option for the AIM keyword as implemented in Gaussian 98. The AIM method was extended and implemented within Gaussian program by Cioslowski.^{19,20} Finally, for an

- | | |
|---|---|
| 1 R = $-\text{N}^+(\text{CH}_3)_3$ | 11 R = $-\text{NO}_2$ |
| 2 R = $-\text{ACNH}$ | 12 R = $-\text{OCH}_3$ |
| 3 R = $-\text{Br}$ | 13 R = $-\text{OEt}$ |
| 4 R = $-\text{CF}_3$ | 14 R = $-\text{OH}$ |
| 5 R = $-\text{CH}_3$ | 15 R = Para-NO_2 |
| 6 R = $-\text{Cl}$ | 16 R = Para-OCH_3 |
| 7 R = $-\text{CHO}$ | 17 R = $-\text{Ph}$ |
| 8 R = $-\text{Et}$ | 18 R = $-\text{Si}(\text{CH}_3)_3$ |
| 9 R = $-\text{F}$ | 19 R = $-\text{t-Bu}$ |
| 10 R = $-\text{NH}_2$ | AMAC R = $-\text{H}$ |

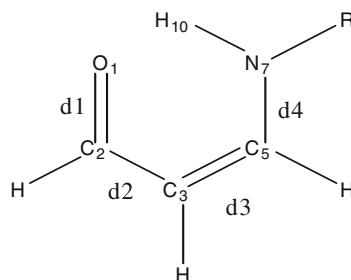


Figure 1. Geometry of AMAC and derivatives.

advanced understanding of the nature of intramolecular interactions, the natural bond orbital (NBO)²¹ analysis was carried out on the B3LYP/6-31G** wave function using the NBO package included in Gaussian 98 suite of program.

3. Results and discussion

3.1 Molecular geometry

The geometry of AMAC and the numbering of the ring atoms and the geometrical parameters of the ring framework of **1–19** are given in figure 1 and in table 1, respectively.

The geometrical parameters showed that the N...O, O...H distances and $\theta_{(N-H...O)}$ in chelated ring are in the range of 2.624–2.733 Å, 1.747–1.929 Å and 124.2–139.3 degree, respectively. It is well known that the geometrical parameters of the HB reflect the strength of the bond. In many cases, there is a clear relationship between these parameters and the strength of hydrogen bond. The smaller the N...O and O...H distances and the larger $\theta_{(N-H...O)}$ angle in the AMAC derivatives, the stronger is intramolecular hydrogen bond. Results in table 1 show that in **1** compound, the $\theta_{(N-H...O)}$ angle is larger and HB is stronger than the other derivatives.

As shown in this table, analysis of bond lengths indicates that r_{C-C} and $r_{C=C}$ in **5, 8, 10, 16, 18, 19** are

shortened and lengthened, respectively, with respect to the AMAC base molecule. Additionally, $r_{C=O}$ in **5, 8, 10, 16, 17, 19** and r_{N-H} in **1–19** are lengthened. These shortening and lengthening of single and double bonds could be attributed to the increasing quantification of π -electron delocalization in the ring of the substituted AMAC, which in turn causes the hydrogen bond to become stronger than that for AMAC. Therefore, among the compounds studied in this work, the simultaneous lengthening of double and shortening of single bonds, is observed in **5, 8, 10, 16, 19**. Alternatively, the main effect of **1–19** substitutions on nitrogen atom is shortening of the N...O distance (except for **7, 8, 18** and **19**) and lengthening of the N–H bond length in **1–19** compared with the corresponding value for AMAC. These structural changes in R-AMAC (R = **1–19**) suggest a stronger hydrogen bond in R-AMAC than that in parent molecule.

3.2 H-bond energies

One of the most important features of intramolecular H-bond is its strength. The intramolecular HB energy plays a significant role in conformational preference and its value mainly depends on the choice of the resonance state. Many authors have devised various methods to estimate the energy of intramolecular HB. In Shuster method,²² it is assumed that the energy difference between the close (with HB) and open

Table 1. The geometrical parameters (r and θ are in Å and °, respectively) and hydrogen bond energies (kJ/mol) of AMAC and its derivatives.

	$r_{C=O}$	r_{C-C}	$r_{C=C}$	r_{C-N}	r_{N-H}	$r_{O...H}$	$r_{N...O}$	θ_{NHO}	E_{HB}	Q
AMAC	1.241	1.436	1.374	1.343	1.019	1.916	2.693	130.6	−33.47	0.164
1	1.234	1.462	1.356	1.390	1.039	1.747	2.624	139.3	−56.76	0.262
2	1.239	1.439	1.368	1.350	1.025	1.899	2.683	130.7	−35.42	0.182
3	1.240	1.439	1.372	1.355	1.030	1.837	2.646	132.7	−43.13	0.182
4	1.239	1.445	1.364	1.362	1.027	1.857	2.664	132.8	−39.53	0.204
5	1.244	1.432	1.378	1.340	1.025	1.872	2.690	134.3	−38.24	0.150
6	1.241	1.437	1.372	1.352	1.030	1.829	2.629	131.6	−44.22	0.176
7	1.235	1.451	1.361	1.369	1.023	1.911	2.705	132.1	−33.68	0.224
8	1.244	1.432	1.378	1.340	1.025	1.879	2.695	134.2	−37.52	0.150
9	1.237	1.443	1.367	1.357	1.026	1.929	2.645	124.2	−33.40	0.196
10	1.244	1.432	1.377	1.342	1.025	1.890	2.678	131.2	−36.69	0.153
11	1.233	1.452	1.360	1.363	1.023	1.916	2.654	126.3	−33.60	0.222
12	1.241	1.436	1.373	1.347	1.027	1.909	2.666	127.9	−34.99	0.169
13	1.241	1.436	1.374	1.346	1.026	1.911	2.668	127.9	−34.75	0.167
14	1.240	1.438	1.372	1.350	1.026	1.917	2.671	127.8	−34.17	0.176
15	1.239	1.443	1.369	1.356	1.027	1.849	2.686	136.3	−40.63	0.191
16	1.243	1.435	1.376	1.347	1.026	1.857	2.692	136.1	−39.81	0.163
17	1.242	1.437	1.374	1.350	1.026	1.859	2.693	135.9	−39.45	0.171
18	1.241	1.436	1.375	1.353	1.028	1.883	2.733	137.7	−36.75	0.173
19	1.244	1.432	1.379	1.340	1.024	1.887	2.703	134.3	−36.62	0.149

(without HB) conformers is equal to HB energy. But this energy gap also contains some conformational contributions and not a direct measure of the HB energy. In recent years, the powerful method of Espinosa²³ is often applied for the estimation of H-bond energy. In this method, the H-bond energies may be estimated from the properties of bond critical points. Espinosa and co-workers have proposed a simple relationship between the hydrogen bond energy and the local electron potential energy density $V(r_{CP})$ at $\rho_{O...H}$: $E_{HB} = 1/2 V(r_{CP})$.

Corresponding to the Abramov's relation²⁴ at the critical point (i.e. $\nabla\rho(r_{CP}) = 0$):

$$G(r_{CP}) = (3/10) (3\pi^2)^{2/3} \rho^{5/3}(r_{CP}) + (1/6) \nabla^2\rho(r_{CP}).$$

The local potential energy density $V(r_{CP})$ can be obtained from the virial equation²⁵:

$$2G(r_{CP}) + V(r_{CP}) = (1/4) \nabla^2\rho(r_{CP}).$$

All values in the realations mentioned above are expressed in atomic units. E_{HB} energies calculated from the potential energy densities of O...H contacts are included in table 1. It is worthy to mention that E_{HB} correlates to the geometrical parameters which are usually assumed to be good descriptors of the H-bond strength. The linear correlation coefficient for the dependency of E_{HB} versus $r_{O...H}$ is 0.985. It means that E_{HB} is a good description of the H-bond strength. Therefore,

E_{HB} could be easily evaluated from O...H bond length, as follow:

$$E_{HB} = 125.81 (r_{O...H}) - 274.38.$$

3.3 Charge density properties

The calculated electron density, ρ , and its second derivative, $\nabla^2\rho$ were used for describing the nature of the intramolecular N-H...O bonds. The calculated electron density (ρ), its Laplacian ($\nabla^2\rho$) at bond critical points and charge density at ring critical point (ρ_{RCP}), its Laplacian ($\nabla^2\rho_{RCP}$) for AMAC and its derivatives are given in table 2. The calculated electron density properties of AMAC and its derivatives demonstrate that O...H bonding has low ρ , (ranging from 0.0311 to 0.0449), and positive $\nabla^2\rho$ values (ranging from 0.0919 to 0.1276). These properties are typical for closed-shell interactions as HBs and indicate electrostatic character of the O...H bondings. The calculated Laplacian at the critical points of N-H bonds in AMAC and its derivatives had negative $\nabla^2\rho$ values, thus pointing out that N-H bonds in AMAC and its derivatives have covalent character. With considering calculated topological parameters, we can conclude that the main effect of substitutions in R positions (in contrary to F group) is an increase in electronic densities at O...H bond critical points (ρ_{BCP}). This fact indicates that the

Table 2. Topological parameters (in a.u.) and frequencies (in cm^{-1}) of stretching (ν) and out of plane bending (γ) mode of N-H group of AMAC and its derivatives.

	$\rho_{O...H}$	$\nabla^2\rho_{O...H}$	ρ_{RCP}	$\nabla^2\rho_{RCP}$	ν_{N-H}	γ_{N-H}	$\Delta\nu$
AMAC	0.0312	0.0925	0.0144	0.0964	3456	787	0
1	0.0449	0.1276	0.0166	0.1142	3164	872	292
2	0.0326	0.0949	0.0146	0.0968	3393	756	63
3	0.0373	0.1068	0.0158	0.1055	3327	817	129
4	0.0351	0.1027	0.0151	0.1017	3366	788	90
5	0.0344	0.0993	0.0150	0.1010	3390	807	66
6	0.0379	0.1094	0.0158	0.1059	3326	800	131
7	0.0315	0.0919	0.0144	0.0949	3431	845	25
8	0.0339	0.0978	0.0149	0.1002	3387	811	69
9	0.0311	0.0930	0.0149	0.0964	3407	778	49
10	0.0334	0.0967	0.0148	0.0978	3395	748	61
11	0.0312	0.0938	0.0147	0.0947	3446	792	11
12	0.0323	0.0942	0.0148	0.0968	3387	753	69
13	0.0321	0.0938	0.0148	0.0964	3392	752	65
14	0.0318	0.0930	0.0147	0.0961	3404	776	53
15	0.0358	0.1035	0.0151	0.1029	3345	867	111
16	0.0353	0.1016	0.0151	0.1024	3355	849	101
17	0.0351	0.1013	0.0151	0.1020	3360	852	96
18	0.0336	0.0951	0.0150	0.0997	3334	859	122
19	0.0334	0.0961	0.0149	0.0992	3404	769	53

hydrogen bond strength upon R substitutions is stronger than that of the non-substituted AMAC (except for F).

Another topic analysed here is the existence of the ring critical point (RCP) for chelated ring of AMAC and its relative. The $\nabla^2\rho_{\text{RCP}}$ is a point of the minimum electron density within the ring surface and a maximum on the ring line. For the systems investigated there are an excellent correlations among these parameters (e.g., $\nabla^2\rho_{\text{RCP}}$ and $\rho_{\text{O...H}}$) with a correlation coefficient of 0.99.

On the other hand, there is a linear relationship between E_{HB} and $\nabla^2\rho_{\text{RCP}}$ at the RCP. The corresponding correlation coefficient amounts to 0.98 (with equation as: $E_{\text{HB}} = -1126.7\nabla^2\rho_{\text{RCP}} + 74.582$). This implies that the properties of the ring critical point values could be very useful to estimate the strength of the intramolecular hydrogen bond. Their values permit us to have a better understanding of these novel correlations. The derived relationships from these graphs empower us to acquire other physically meaningful results.

In order to better elucidate hydrogen-bond strength, vibrational frequencies for all of derivatives were calculated. It is well known that the strengthening of hydrogen bond causes frequencies of NH stretching mode shift to lower frequencies (red shift, figure 2). Corresponding wave numbers of the above mode have been listed in table 2.

Table 2 shows the shifts in frequency ($\Delta\nu$) of the proton donating bonds for the compounds investigated here. These shifts correlate with the H-bond energies and are the greatest for the strongest hydrogen bonds (for R = 1). The correlation coefficient between H-bond energy and $\Delta\nu$ for all of the compounds analysed here amounts to 0.95. Therefore, E_{HB} can be easily evaluated from $\Delta\nu$, as follows:

$$E_{\text{HB}} = -0.0839\Delta\nu - 31.196.$$

Moreover, table 2 shows that the longer $r_{\text{N-H}}$ proton donating bond for the AMAC and its derivatives

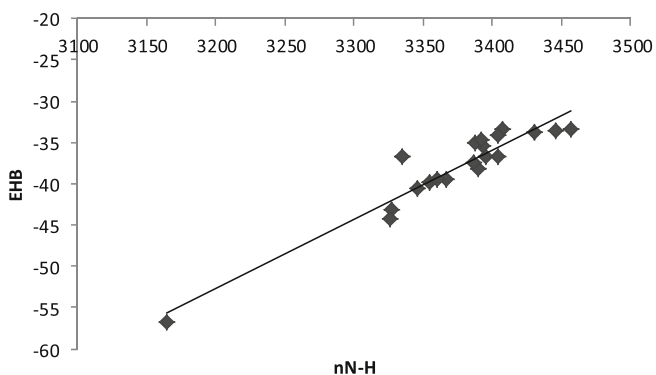


Figure 2. The correlation between the E_{HB} energy (kJ/mol) and $\nu_{\text{N-H}}$ (in cm^{-1}).

is connected with the greater corresponding stretching frequency shift as a result of H-bond formation.

3.4 NBO analysis

The natural bond orbital (NBO) analyses²⁶ were applied to evaluate the hydrogen bond strength in the ring of AMAC and its derivatives. Table 3 shows some of the significant donor-acceptor interactions and their second order perturbation energies $E^{(2)}$. In the NBO analysis of hydrogen bond system, the charge transfer between the lone pairs of proton acceptor and antibonds of the proton donor is the most important parameter. The results of NBO analysis illustrate that in the ring structure of AMAC and its derivatives, two lone pairs of oxygen atom (n_{O}) participate as donors and the $\sigma^*_{\text{N-H}}$ interactions behave as acceptors in relatively strong intramolecular charge transfer interactions with the energy values presented in table 3. The energy corresponds to the $n_{\text{O}} \rightarrow \sigma^*_{\text{N-H}}$ interaction which is connected with the maximum $n_{\text{O}} \rightarrow \sigma^*_{\text{N-H}}$ overlap leading to a linear, or nearly so, geometry of the N-H...O hydrogen-bonded system. Hydrogen bonding causes an increase of the occupancy of the $\sigma^*_{\text{N-H}}$ antibond orbital and furtherer the weakening and lengthening of the N-H bond. These orders of energy values again support calculated intramolecular hydrogen bonds strength values in AMAC and its derivatives. It is worth mentioning that NBO energy connected with $n_{\text{O}} \rightarrow \sigma^*_{\text{N-H}}$ overlap nicely correlates with other geometrical and topological parameters. Moreover, we found out that there is a good correlation between E_{HB} and $n_{\text{O}} \rightarrow \sigma^*_{\text{N-H}}$ with correlation coefficient of 0.95. These kinds of correlations are important, because they permit us to quantitatively dictate the strength of such interactions and provide a physical explanation for the process.

Natural bond orbital analysis shows that there is a strong negative hyperconjugative interactions $n_{\text{O}} \rightarrow \sigma^*_{\text{C-C}}$ in the studied molecules (table 3). For example, the second order energies for **11** derivativ is 59.79 kJ/mol. This interaction weakens the $\text{C}_2\text{-C}_3$ sigma bond and elongates the C-C bond length in these molecules. In addition, it is found that AMAC and its derivatives are characterized by a very strong $n_{\text{N}} \rightarrow \pi^*_{\text{C=C}}$ delocalization.

3.5 Resonance

The π -electron delocalization is a well known phenomenon that exists in simple and complex molecules and influences their physical and chemical properties. The π -electron delocalization is inseparable from other similar phenomenon, such as aromaticity which is frequently discussed and analysed.²⁷ The parameter of

Table 3. NBO analysis of AMAC and its derivatives. This includes the second order perturbation energy (in kJ/mol) of some important orbital interactions.

	n_{σ^*N-H}	$\Delta E_{nN \rightarrow \pi^*C=C}$	$\Delta E_{nO \rightarrow \sigma^*N-H}$	$\Delta E_{nO \rightarrow \sigma^*C-C}$
AMAC	0.039	245.10	39.90	54.47
1	0.068	110.91	83.69	50.58
2	0.056	189.29	42.12	54.64
3	0.056	139.21	52.00	51.29
4	0.051	196.82	50.49	54.05
5	0.051	257.36	49.78	51.37
6	0.058	166.59	53.93	50.20
7	0.046	179.57	41.03	57.86
8	0.052	258.28	48.94	51.67
9	0.048	136.99	32.15	56.94
10	0.057	241.70	45.72	51.71
11	0.043	175.43	37.10	58.91
12	0.057	172.24	38.85	54.09
13	0.057	176.81	38.77	54.01
14	0.054	164.04	37.18	54.93
15	0.055	**	56.06	52.96
16	0.054	**	54.93	51.37
17	0.054	**	54.01	52.13
18	0.049	235.63	49.91	52.59
19	0.050	260.17	48.86	51.83

such delocalization can be calculated from the following equation²⁸:

$$Q = (d4 - d1) + (d2 - d3), \quad (1)$$

where $d1$, $d2$, $d3$ and $d4$ are bond lengths (see figure 1). The values of Q -parameters for the systems probed here are given in table 1. As it is obvious from table 1, the greatest value of Q -parameter is 0.262 for $R = 1$ and the lowest is 0.149 for $R = 19$.

3.5a Model of HOMA: Harmonic oscillator measure of aromaticity (HOMA) which is a geometrical indicator of a local aromaticity²⁹ can be expressed by the following equation:

$$HOMA = 1 - \frac{1}{n} \sum_{j=1}^n \alpha_i (R_{opt,i} - R_j)^2,$$

where n represents the total number of bonds in the molecule and α_i is normalization constant. Using C=O, C-C and C-N bonds: $R_{opt, C=O} = 1.265 \text{ \AA}$, $R_{opt, C=C} = 1.388 \text{ \AA}$ and $R_{opt, C-N} = 1.334 \text{ \AA}$, $\alpha_{C=O} = 157.38$, $\alpha_{C-C} = 257.7$ and $\alpha_{C-N} = 93.52$ gives $HOMA = 0$ for a model non-aromatic system and $HOMA = 1$ for the system with all bonds equal to the optimal value $R_{opt,i}$, assumed to be realized for fully aromatic systems.³⁰ The higher is the HOMA value, the more 'aromatic' is the ring in question and, hence, the more delocalized π -electrons of the system. Comparison of local aromaticity systems with the parent molecule in all derivatives

elucidates the aromaticity order for AMAC derivatives. Table 4 illustrates the main effect of **16**, **19**, **5**, **8**, and **10** groups on the R substitution in AMAC, indicating an increase in local aromaticity (enhancement of HOMA index with respect to $R=H$).

Our calculated results show that there is no linear correlation between HOMA versus E_{HB} . Additionally, there is an excellent linear correlation coefficient between HOMA and Q with correlation coefficient of 0.99 (see figure 3) which indicates as the HOMA values are increasing, the Q values are decreasing, deriving the following equations;

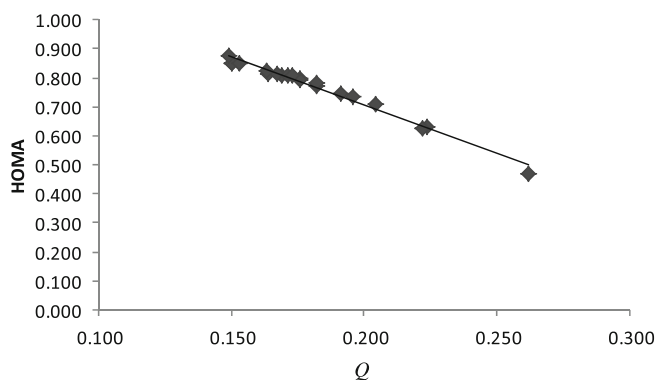
$$HOMA = -3.32 Q + 1.37.$$

3.5b Dependences between substituent constants and selected parameters of systems: Experimentally different substitution constants have been utilized to investigate the substituent effect, namely, σ^+ , σ^- , F , R^+ and R^- .³¹ These substituent constants are numerically characterizing mutual electron interaction between a given substituent and the para-placed reactivity centre proceeding through the aromatic ring. The σ^+ is a substituent constant originally estimated from solvolysis of dimethyl phenyl carbinyl chloride derivatives in which substitution is located on para position. In other words, σ^+ values are estimated for centres which introduce a positive charge onto its carrier ring. σ^- values were originally estimated from pK values of para substituted phenols and anilines. In other words, these values have

Table 4. Substituent constants corresponding to the substituent's considered in this work and HOMA parameter.

	σ^+	σ^-	F	R^+	R^-	HOMA
AMAC	0.00	0.00	0.00	0.00	0.00	0.814
1	0.41	0.77	0.86	-0.45	-0.09	0.470
2	-0.60	-0.46	0.31	-0.91	-0.77	0.774
3	0.15	0.25	0.45	-0.30	-0.20	0.781
4	0.61	0.65	0.38	0.23	0.27	0.708
5	-0.31	-0.17	0.01	-0.32	-0.18	0.851
6	0.11	0.19	0.42	-0.31	-0.23	0.799
7	0.73	1.03	0.33	0.40	0.70	0.633
8	-0.30	-0.19	0.00	-0.30	-0.19	0.851
9	-0.07	-0.03	0.45	-0.52	-0.48	0.733
10	-1.30	-0.15	0.08	-1.38	-0.23	0.849
11	0.79	1.27	0.65	0.14	0.62	0.626
12	-0.78	-0.26	0.29	-1.07	-0.55	0.810
13	-0.81	-0.28	0.26	-1.07	-0.54	0.813
14	-0.92	-0.37	0.33	-1.25	-0.70	0.792
15	0.04	0.31	0.26	-0.22	0.05	0.744
16	**	**	**	**	**	0.825
17	-0.18	0.02	0.12	-0.30	-0.10	0.806
18	0.02	**	0.01	0.01	**	0.810
19	-0.26	-0.13	-0.09	-0.17	-0.04	0.875

been evaluated for those centres having lone electron pairs, e.g. OH or NH₂ group, so the centre which introduces a negative charge onto its carrier ring.³² F values reflect field/inductive properties of a given substituent, while R^+ and R^- are the resonance constants obtained for suitable centres of reactivity. A large positive value of a given constant implies high electron-withdrawing power by inductive and/or resonance effect, relative to the hydrogen atom; for the same token, a large negative value of a given constant implies high electron-donating power relative to the hydrogen atom. The values σ^+ , σ^- , F , R^+ and R^- of the substituent constants for the substituent studied in this work have been compiled in table 4.

**Figure 3.** The correlation between the Q and HOMA parameters.

3.5c Systems substituted at position R of AMAC: It should be mentioned that all changes observed for collected parameters have been derived directly from the influence of the substituent R onto the electronic structure of AMAC moiety. This influence proceeds in two possible manners; firstly, there is a mesomeric effect in which a substituent is potentially involved in π -electron communication with the AMAC moiety, and secondly, there is a field/inductive effect, which mainly concerns the substituted N atom of AMAC. In the latter case, the electronic effect depends primarily on electronegativity of the group attached to the quasi-ring. It can be stated that the field/inductive effect is in general weak in the case of substituents such as CH₃ ($F = 0.01$, see table 4). This can be implied by relatively small values of the corresponding substituent constant F . In general, all these substituents can be treated as electron-withdrawing ones (by means of field/inductive effect) with all having positive values of F . We expect that this effect will be only slightly influencing the quasi-aromaticity and H-bonding in the quasi-ring. In the case of mesomeric (resonance) effect, the situation is more complicated, since in this case the inner resonance effect within the quasi-ring has to be additionally accounted for. Therefore, it is worth to take a closer look into the resonance structures of substituted AMAC system. In figure 4, the resonance effect proceeding in this system could be divided into three separated model situations (three cases) illustrating three

mesomeric effects which are cooperating or competing between each other. The first is a resonance effect taking place within the quasi-ring of MPT moiety ($1a \leftrightarrow 1b$). In this case, the substituent does not participate in π -electron delocalization and the effect proceeds apart from the character of attached substituent.

This is the fully illustrated case of unsubstituted AMAC ($R=H$), which leads to partial delocalization of π -bonds, favouring H-bonding. Additionally, the stronger HB in AMAC causes the N–H and O...H bond lengths come closer to each other. The second case corresponds to the situation in which the substituent attached to AMAC has electron-withdrawing properties (by means of mesomeric effect) and is participating in electron delocalization within the whole system. It is possible to postulate, that both effects are cooperating (there is a direct transition between canonical structures of effects $1b$ and $2b$) producing weaker HB. For NH_2 substituent, the π -electron donation can be partially inhibited by the σ -electron accepting character of the N atom.³³ For most systems with electron-withdrawing substituents (figure 4) a decrease in the delocalization and quasi-aromatic character of the AMAC quasi-ring reflected by the corresponding values of aromaticity indices can be observed (see table 4 and Q indices in table 1).

In the third case of electron-donating substituents (structures $3a \leftrightarrow 3b$ in figure 4), the effect of resonance in the HB is strongly limited to Cl, CH₃ substituents. The only possible effect is the introduction of partial negative charge into one of the carbon atoms. Indeed, the participation of structure $3b$ strengthens the HB, since the negative charge formally located on the C atom should block the AMAC. The strengthening of the

HB for electron-donating substituents can be realized from the $r_{O...H}$, Q , E_{HB} and HOMA values compiled in table 1 and table 4.

In Summary, we have shown that, in the AMAC substituted at position R , the interaction between substituents and quasi-ring is proceeding mainly through the resonance effect favouring HB in the case of electron-donating substituents and disfavoring HB for electron-withdrawing groups. The effect of substitutions can be quantified by the use of substituent constants estimated for suitable chemical groups. All findings can be interpreted as, the H atom in quasi-ring adopts a behaviour similar to N...O moiety, which can introduce a negative charge onto its carrier ring. This conclusion confirmed that H atom shares easily its electronic charge adopting positive charge.

4. Conclusions

We examined the intramolecular hydrogen bondings for AMAC and its derivatives using B3LYP level of theory at the standard 6-31G** basis set. The results obtained from DFT calculations and the topological parameters derived from the Bader theory suggest that stronger hydrogen bond can lead to shortening of the N...H distance. Our findings confirm that π -electron delocalization for the chelated ring created by the H-bond formation exists and the topological parameters derived from the theory of Bader may be applicable for estimation of H-bond strength. Our calculated RCPs values are useful descriptor of the strength of intramolecular H-bonds. The electron withdrawing and electron donating substituents may influence the π -electron delocalization. However, E_{HB} energy calculated from the topological parameters may be treated as the H-bond energy, and well correlates to the pertinent HB strength parameters. Moreover, the calculated electron density and Laplacian properties of AIA and its derivatives illustrate that O...H bonding in all molecules has lower ρ and positive $\nabla^2\rho$ values, which is typical for closed-shell interactions indicating electrostatic character of the O...H bondings. Meanwhile, it was concluded that substituents attached to the AIA moiety influence both the intramolecular HB as well as the quasi-aromatic character of the quasi-ring. Furthermore, NBO analysis confirmed that there is a strong negative hyperconjugative interactions $n_O \rightarrow \sigma^*_{C2-C3}$ in the studied molecules.

References

1. Raissi H, Jalbout A F, Nasser M A, Yoosefian M, Ghassi H and Hameed A J 2008 *Int. J. Quant. Chem.* **108** 1444

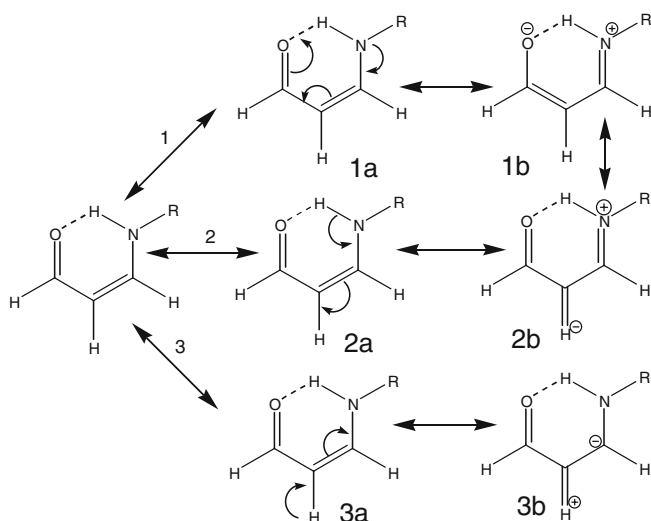


Figure 4. Schematic representation of resonance (mesomeric) effect in AMAC systems substituted at position R .

2. Raissi H, Jalbout A F, Fazli M, Yoosefian M, Ghassi H, Wang Z and De Leon A 2009 *Int. J. Quant. Chem.* **109** 1497
3. Fazli M, Jalbout A F, Raissi H and Yoosefian M 2009 *J. Theor. Comput. Chem. (JTCC)* **8** 713
4. Raissi H, Jalbout A F, Yoosefian M, Fazli M, Nowroozi A, Shahini M and De Leon A 2010 *Int. J. Quant. Chem.* **110** 821
5. Grabowski S J 2001 *J. Mol. Struct.* **562** 137
6. Raissi H, Nadim E S, Yoosefian M, Farzad F, Ghiamati E, Nowroozi A R, Fazli M and Amoozadeh A 2010 *J. Mol. Struct. THEOCHEM* **960** 1
7. Nadim E S, Raissi H, Yoosefian M, Farzad F and Nowroozi A R 2010 *J. Sulfur Chem.* **31** 275
8. Raissi H, Yoosefian M, Mollania F, Farzad F, Nowroozi A R and loghmaninejad D 2011 *J. Comput. Theor. Chem.* **966** 299
9. Nazir H, Yildiz M, Yilmaz H, Tahir M N and Ulku D 2000 *J. Mol. Struct.* **524** 241
10. Gilli F, Belluci V, Ferretti V and Bertolasi V 1989 *J. Am. Chem. Soc.* **111** 1023
11. Barone V, Palma P and Sanna N 2003 *Phys. Lett.* **381** 451
12. Nowroozi A R, Raissi H and Farzad F 2005 *J. Mol. Struct. (THEOCHEM)* **730** 161
13. Buemii G, Zuccarello F, Venuvanalingam P and Ramalingam M 2000 *Theor. Chem. Acc.* **104** 226
14. Gilli P, Bertolasi V, Pretto L and Gilli G 2002 *J. Am. Chem. Soc.* **124** 13554
15. Raissi H, Moshfeghi E and Farzad F 2005 *Spectro Chimica, Acta Part A* **62** 1004
16. Raissi H, Moshfeghi E, Jalbout A F, Hosseini M S and Fazli M 2007 *Int. J. Quant. Chem.* **107** 1835
17. Frisch M J, Trucks G W, Schlegel H B, Scuseria G E, Robb M A, Cheeseman J R, Zakrzewski V G, Montgomery J A Jr, Stratmann R E, Burant J C, Dapprich S, Millam J M, Daniels A D, Kudin K N, Strain M C, Farkas O, Tomasi J, Barone V, Cossi M, Cammi R, Mennucci B, Pomelli C, Adamo C, Clifford S, Ochterski J, Petersson G A, Ayala P Y, Cui Q, Morokuma K, Malick D K, Rabuck A D, Raghavachari K, Foresman J B, Cioslowski J, Ortiz J V, Stefanov B B, Liu G, Liashenko A, Piskorz P, Komaromi I, Gomperts R, Martin R L, Fox D J, Keith T, Al-Laham M A, Peng C Y, Nanayakkara A, Gonzalez C, Challacombe M, Gill P M W, Johnson B, Chen W, Wong M W, Andres J L, Gonzalez C, Head-Gordon M, Replogle E S and Pople J A, Gaussian, Inc., Pittsburgh PA, 1998
18. Becke A D 1993 *J. Chem. Phys.* **98** 5648
19. Cioslowski J, Nanayakkara A and Challacombe M 1993 *Chem. Phys. Lett.* **203** 137
20. Cioslowski J 1992 *Chem. Phys. Lett.* **194** 73
21. Glendening E D, Reed A E, Carpenter J E, Weinhold F, NBO, Version 3.1, Gaussian, Inc., Pittsburgh PA, 1992
22. Schuster P, G Zundel and Sandorfy C 1976 Hydrogen bonding, North Holland, Amsterdam
23. Espinosa E, Molins E and Lecomte C 1998 *Chem. Phys. Lett.* **285** 170
24. Abramov Y A 1997 *Acta Crystallogr. A* **53** 264
25. Schleyer P V R 2005 *Chem. Rev.* **105** 3433
26. Reed A E, Curtis L A and Weinhold F A 1988 *Chem. Rev.* **88** 899
27. Krygowski T M and Cyranski M 2001 *Chem. Rev.* **101** 1385
28. Gilli G, Bellucci F, Ferretti V, Bertolasi V 1989 *J. Am. Chem. Soc.* **111** 1023
29. Krygowski T M 1993 *J. Chem. Inf. Comput. Sci.* **33** 70
30. Julg A and Francoise P 1967 *Theor. Chim. Acta* **7** 249
31. Hansch C, Leo A and Taft R W 1991 *Chem. Rev.* **91** 165
32. Hammett L P 1970 *Physical Organic Chemistry* (New York: McGraw-Hill)
33. Fore's M, Duran M, Sola' M 2000 *Chem. Phys.* **260** 53